

# Effect of interparticle interaction on localization in a nonideal crystal with a narrow band

Yu. Kagan and L. A. Maksimov

Zh. Eksp. Teor. Fiz. **88**, 992–1000 (March 1985)

The interaction between particles can cause either localization or delocalization. Delocalization occurs after a threshold is reached and requires a finite particle density which depends on how nonideal the crystal is. The onset of localization with increasing particle density is related to self-localization in an ideal crystal { Yu. Kagan and L. A. Maksimov, Zh. Eksp. Teor. Fiz. **87**, 348 (1984) [Sov. Phys. JETP **60**, 201 (1984)] }. Phase diagrams are constructed to illustrate the localization and delocalization regions as functions of the temperature, the defect concentration, and the particle concentration. Phase transitions to a self-localization state are predicted as the temperature is raised.

## 1. INTRODUCTORY COMMENTS

For motion in a narrow band in a crystal the region in which particles interact strongly with defects and with each other typically has a large radius. We assume that the interaction is repulsive in both cases, and we assume, exclusively for simplicity, that the two interactions are identical, described by the power law

$$U(r) = U_0(a_0/r)^\alpha, \quad \alpha > 3 \quad (1)$$

[the volume of the unit cell of the lattice is  $(4/3)\pi a_0^3$ ]. If the band width  $\Delta$  satisfies the inequality

$$\Delta/U_0 \ll 1, \quad (2)$$

it is easy to see that, even for states at the center of the band, the potential and kinetic energies are equal,

$$U(R_0) = \Delta, \quad (3)$$

at a radius

$$R_0 \gg a. \quad (4)$$

This result means that each particle or point defect is surrounded by a large "exclusive volume" which the other particle must "circumvent" in the course of scattering. The volume is filled with such spheres at a concentration

$$x_0 = (a_0/R_0)^3 \ll 1. \quad (5)$$

We initially assume that the particle concentration  $x$  is negligible. At a static-defect concentration  $y_c = \nu y_0 \ll 1$  ( $\nu > 1$  is a numerical factor, and  $y_0 = x_0$ ), absolute localization will then occur, i.e., localization for all the energy states in the band. In the absence of inelastic processes this localization is a quantum process (Anderson localization<sup>1</sup>). By virtue of inequality (4),  $y_c$  lies very close to  $\tilde{y}_c$ , the point of purely classical localization of the percolation type (Ref. 2).

We now consider the opposite case, in which there are no defects, and the particle concentration is finite. We assume  $T > \Delta$ ,  $U_x$  (where  $U_x$  is the characteristic interaction energy of the particles at the concentration  $x$ ); at  $x \ll 1$ , therefore, the particles clearly obey classical statistics. In contrast with the preceding case, in which the particle concentration reaches the region  $x \sim x_0$ , the gaseous diffusion regime gives

way to a liquid regime, but no localization of any sort occurs. An irreversible escape of a particle from a particular spatial volume now results from many-particle excitations, which cause the particle to diffuse in energy and which alter the local potential relief.

As the particle concentration is increased further, however, we enter a region in which the size of the relative shift of the levels in adjacent unit cells due to the interaction of the particles at an intermediate distance begins to exceed  $\Delta$ . The corresponding characteristic concentration  $x_{00}$  can be found from an expression analogous to (5), by replacing  $R_0$  by the radius  $R_{00}$  defined by

$$a |\nabla U|_{r=R_{00}} = \gamma \Delta \quad (6)$$

( $\gamma > 1$  is a numerical factor).

In this concentration range, in the absence of an interaction with phonons, in a randomly distributed system of particles ( $T > U_x$ ), an infinite immobile cluster forms, in which both single-particle and many-particle motions are suppressed.<sup>2</sup> The principal reason for this situation is the discrete nature of the space which is imposed by the periodic structure of the ideal lattice. In contrast with the case of diffusion in a liquid, this periodic structure requires that a particle undergo a finite displacement to reach resonance also and makes available a finite number of resonant paths,  $z$ . Particles which do not belong to the infinite cluster remain capable of diffusing through interactions with each other. (Their interaction with the particles of the immobile cluster is an elastic interaction.<sup>2</sup>) At a concentration  $x_c = \eta x_{00}$  ( $\eta \sim 2$ ), however, the strength of the immobile cluster, which is evidently serving as a static defect structure, reaches a level such that the volume which is kinetically accessible to free particles contracts to a critical size at which the particles can no longer escape to infinity. As a result, complete localization occurs in an ideal crystal without static defects, solely because of the interaction of the diffusing particles with each other. We wish to stress that we are talking here about the high-temperature limit; a further increase in the temperature will not change  $x_c$ .

Localization of this type and also delocalization caused by phonons<sup>3</sup> have been detected experimentally by Mikheev *et al.*<sup>4-6</sup> in the diffusion of He<sup>3</sup> in a He<sup>4</sup> crystal.

## 2. ROLE OF THE INTERPARTICLE INTERACTION IN LOCALIZATION

We now consider the general case ( $y \neq 0, x \neq 0$ ), and we analyze the effect of the interparticle interaction on the picture of localization in a crystal with static defects. We begin the study with the high-temperature limit.

We assume  $y > y_c, \bar{y}_c$ . When, with increasing concentration  $x$ , the interaction between particles comes into play, an energy diffusion arises in the potential relief created by the static defects. The particle no longer exhibits a fixed energy level; on the contrary, diffusion now occurs, in principle, in an energy band  $\Delta E \sim U_y > \Delta$ . As a consequence, the quantum localization due to phase relaxation is eliminated (Ref. 7, for example), and in addition the increase in the size of the region of the crystal which is kinetically accessible to particles eliminates classical localization. An upper limit is set on the concentration in the delocalization region by the self-localization of particles. It is easy to understand that the presence of defects effectively increases the strength of the immobile cluster at a given  $x$  and simultaneously lowers the critical concentration for self-localization. The upper boundary of the delocalization region,  $\bar{x}$ , is determined by the simple relation

$$\bar{x} + y \approx x_c. \quad (7)$$

Actually—and this is an important point—the density  $\bar{x}$  in region in which localization is eliminated is also bounded below. The reason is that energy diffusion arises after a threshold value of  $x$  is reached. Let us examine this question in more detail.

At  $y > y_c$ , all the single-particle states are localized. Outside the critical concentration interval, the linear dimension of the localization region of the wave function,  $l$ , can be estimated from the condition that the shift of the band in the potential relief of the impurities be comparable in magnitude to the width of the band:

$$l|\nabla U| \approx \Delta.$$

We thus have the approximate result

$$l(y) \approx R(y) (y_0/y)^{\alpha/3}, \quad R(y) = a_0/y^h. \quad (8)$$

It follows that

$$R(y) > l \gg a; \quad (9)$$

this is a consequence of the large-scale nature of the potential relief created by the defects. The second inequality is violated only at  $y \sim y_{00} = x_{00}$ , where  $l \sim a$ . Let us consider two particles which are in localized states and separated by a distance  $R \gg 1$ . The amplitude for a transition of this pair with a change in the state of each of the particles is determined by the matrix element of the interaction:

$$\frac{\partial^2 U(R)}{\partial R_j \partial R_k} \rho_{1j} \rho_{2k}, \quad \mathbf{R}_{12} = \mathbf{R} + \rho_1 - \rho_2. \quad (10)$$

The dipole matrix element effectively couples localized states separated by an energy

$$\omega(y) \approx \Delta / (l(y)/a). \quad (11)$$

The matrix element itself is given in order of magnitude by

$$V(R) \approx U''(R) l^2. \quad (12)$$

It is easy to see that at distances ( $R$ ) between the particles for which the inequality

$$V(R) \ll \omega(y) \quad (13)$$

holds the probability for the occurrence of a resonant two-particle transition is negligible. If the concentration  $x$  is such that inequality (13) holds at the characteristic distance  $R(x)$  between particles, then no energy excitation can escape from a bounded volume of the crystal. As a consequence, there is no energy diffusion with an irreversible escape of the phase from a given region, and the role of the interaction between particles reduces to a renormalization of the states. In the absence of an energy diffusion, on the other hand, localization persists, and the macroscopic mass diffusion coefficient is  $D = 0$ . The question of maintaining localization when a short-range interaction between particles comes into play was first discussed in Ref. 8.

A localized wave function formally has a nonzero overlap integral with  $(1/a)^3$  states, for which the distance between levels is far smaller than (11). It can be shown, however, that the matrix element for a transition to this fine structure in the level within an interval  $\omega$ , which clearly requires consideration of higher multipoles than (10), decays far more rapidly than does the corresponding decrease in the distance between levels.

We also note that, under condition (13), the amplitude of the many-particle transition decreases exponentially with the number of particles involved in the transition (see the corresponding analysis in Ref. 2), rendering the probability for a resonant process for such transitions (the agreement of the initial and final energies within the transition amplitude) even smaller.

Inequality (13) is evidently violated only at a finite concentration  $x$ , so that the delocalization of particles due to their interaction does in fact require that a threshold be reached.

The lower boundary of the delocalization region,  $\bar{x}$ , is determined by a relation of the type

$$V(R(x)) = \xi \omega(y), \quad (14)$$

where the numerical factor  $\xi$  requires a special determination. Using (11), (12), (8), and (1), we find the approximate result

$$\bar{x} = \xi_1 y_{00} (y/y_{00})^{3(\alpha+1)/(\alpha+2)}. \quad (15)$$

In deriving (15) we have assumed that the parameters of the problem satisfy the condition  $V(x_{00}) > \omega(x_{00})$  (Ref. 2). The opposite case requires special study. It follows from the form of (15) that the  $y$  dependence of  $\bar{x}$  is approximately cubic, and the line  $\bar{x}(y)$  is intersected even at  $\bar{x} < y$ .

As  $y$  approaches  $y_c$ , this law changes to a critical dependence

$$\bar{x} \propto (y - y_c)^\sigma. \quad (16)$$

The reason is that at the critical point  $y_c$  the length  $l$  becomes infinite [it should be kept in mind that representation (8) and expansions (10) and (12) are inapplicable]. At  $y < y_c$  the diffu-

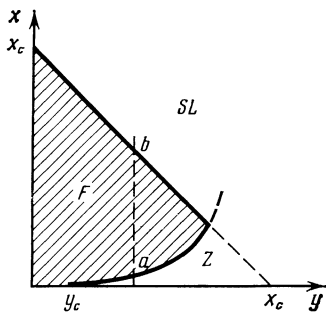


FIG. 1

sion coefficient is  $D \neq 0$ , even in the limit  $x \rightarrow 0$ , and an increase in the particle concentration  $x$  does not qualitatively change the diffusion picture until we reach the self-localization region. On the whole, therefore, the  $(x, y)$  phase diagram will be as shown in Fig. 1, where we are using (7), (15), and (16). The hatched region is the region in which the macroscopic diffusion coefficient is nonzero. Along the line  $ab$  (Fig. 1) the diffusion coefficient initially increases as we move away from point  $a$ ; it goes through a maximum, and then there is a liquid diffusion regime, with  $D$  decreasing with increasing  $x$ . At point  $b$  we have  $D = 0$  as a result of self-localization.

As long as there is no interaction with phonons, the phase diagram at  $T > U_x$  will not change as  $T$  is increased. When the interaction with phonons is taken into account, a phonon-stimulated delocalization occurs in the unhatched region of the phase plane. The interaction with phonons is also important for the part of the hatched region directly adjacent to the boundaries  $\bar{x}(y)$  and  $x(y)$ , causing an increase in  $D$  with increasing  $T$  (Refs. 2 and 3). In the inner part of the hatched region, far from the boundaries, the interaction with phonons causes  $D$  to decrease with increasing  $T$ .

### 3. PHASE DIAGRAM AT $T = 0$

We now consider the corresponding phase diagram for  $T = 0$ , assuming that the particles obey Fermi statistics. We note at the outset that the diagram must be fundamentally different from that in Fig. 1, since now we are dealing with localization in the ground state, while at high temperatures  $T$  the identical population of all the statistically allowed energy states plays a decisive role in the localization.

Assuming that the interaction law in the form in (1) again holds, we find the following result for the amplitude of the scattering of a particle by an impurity in the limit  $E \rightarrow 0$  (the scattering length;  $\alpha > 3$ ):

$$f \approx a(U_0/\Delta_0)^{1/\alpha-2}, \quad \Delta \approx 2z\Delta_0 \quad (17)$$

( $z$  is the number of equivalent sites in the first coordination sphere). A situation in which the impurity is gaseous prevails under the condition

$$y \ll y_*, \quad y_* = (a_0/f)^3 \ll y_0. \quad (18)$$

In the interval of concentrations  $y$  obeying (18), the energy threshold for the localization is found from the Ioffe-Regel'-Mott condition

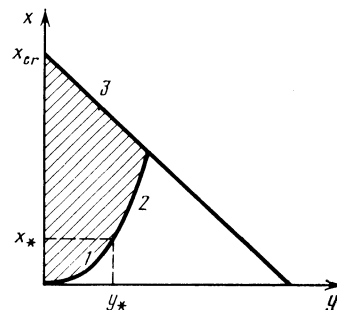


FIG. 2

$$L \approx \lambda. \quad (19)$$

Here  $L = 1/4\pi f^2 n_{im}$  is the mean free path, and  $\hbar$  is the wavelength of the particle. It is easy to see that the condition  $\hbar \gg f$  holds at the delocalization threshold in the gaseous region, (18), and the scattering amplitude retains its limiting value, (17). From (19) we directly find the critical particle concentration:

$$x \approx 4y_*(y/y_*)^3. \quad (20)$$

By virtue of (18), on this critical curve we have  $x \ll y$ , and the interaction between particles plays no substantial role. Consequently, the dependence  $x \sim y^3$  is universal (curve 1 in Fig. 2).

The boundary of the region in which the impurities are gaseous,  $y \approx y_*$ , corresponds on the critical curve to the region in which the transition from a gas of particles to a Fermi liquid occurs ( $x \sim x_* = y_*$ ). Accordingly, at  $y > y_*$ , not only does the nature of the scattering by impurities at the delocalization threshold change, but also the interaction of particles with each other simultaneously becomes important.

At  $y \gg y_*$  we have

$$\eta = U_y / \frac{\hbar^2}{2m \cdot R^2(y)} = \left(\frac{y}{y_*}\right)^{(\alpha-2)/3} \gg 1 \quad \left(\frac{\hbar^2}{2m \cdot a_0^2} \approx \Delta_0\right), \quad (21)$$

and the potential relief which arises is semiclassical. In the "unit cell" per impurity which is characteristic of this potential relief, the number of single-particle levels is

$$N \sim 10^{-4} \eta^{3/2}. \quad (22)$$

The penetrability of the characteristic potential barrier with respect to a transition between these and lower levels is determined by a factor  $e^{-S}$ , where  $S \sim \eta^{1/2}$ . It is easy to see that the probability that discrete levels in neighboring potential wells coincide within the transition amplitude is small, and the states in this part of the spectrum are localized. Actually, delocalization arises in the one-particle problem only at an energy on the order of  $U_y$ . The corresponding threshold energy is

$$\varepsilon_c = \beta U_y. \quad (23)$$

The value of the constant  $\beta$  is approximately equal to the corresponding quantity determined for the threshold for classical percolation in the potential relief under considera-

tion (Ref. 9, for example). The quantum corrections to this quantity for interference effects,  $(\hbar^2/L)^2 \sim \eta^{-1}$ , and for tunneling are small, on the order of the parameter  $\eta^{-1}$ . If we ignore the interaction between particles, we can find the critical concentration directly from (23):

$$x \approx 10^{-1} \beta^{3/2} y_* (y/y_*)^{\alpha/2}. \quad (24)$$

Consequently, for a noninteracting Fermi gas the cubic  $y$  dependence at  $y < y_*$  gives way to a  $x \sim y^{a/2}$  at  $y > y_*$  (curve 2 in Fig. 2).

It can be concluded from (24), however, that on the critical curve we have  $x \gg y$  at  $y \gg y_*$ . If the interaction between particles is comparable in magnitude to that between particles and impurities, it follows that near curve 2 both Fermi-liquid effects and correlation effects will be important (there is an effective "screening" of the impurity potential). When correlation effects are predominant, the exponent  $\alpha/2$  in (24) is replaced by  $\kappa$ , where

$$1 < \kappa < \alpha/2.$$

If we not set  $y = 0$  and arbitrarily increase  $x$ , we find that a certain concentration  $x_{cr} \gg x_*$  the subsystem of particles undergoes a transition to a crystalline state, accompanied by the formation of a regular sublattice. The transition concentration can be determined from the relation between the kinetic and potential energies (on the liquid side),

$$T_{kin}/U_x \sim (x_*/x)^{(\alpha-2)/3},$$

or from the ratio of the square displacement  $\xi^2$  of a particle in the crystal sublattice to the square distance between particles,  $R^2(x)$ ,

$$\xi^2/R^2(x) \sim (x_*/x)^{(\alpha-2)/6}.$$

These two relations leads formally to

$$x_{cr} = \mu x_*, \quad (25)$$

where the numerical parameter is  $\mu \gg 1$ . The small value of  $x_*$  in (18) presupposes that crystallization occurs at  $T = 0$  at a low particle concentration, i.e., that we have  $x_{cr} \ll 1$  and  $R(x_{cr}) \gg a$ . In this case we have  $\xi > a$ ; in other words, the particles in the crystalline phase are smeared over regions large in comparison with the volume of the unit cell of the host.

The concentration  $x_{cr}$  varies comparatively slightly over the  $y$  interval up to the point at which the crystallization

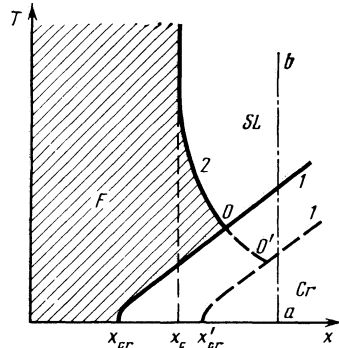


FIG. 3

line  $x_{cr}(y)$  (curve 3 in Fig. 2) crosses curve 2 in Fig. 2. The continuation of the crystallization line formally intersects the abscissa at  $y \approx x_{cr}$ , because of the formation of a common, generally disordered, lattice of particles and impurities.

As a result, the diffusion coefficient at  $T = 0$  on the  $(x, y)$  plane is nonzero only on the hatched region in Fig. 2. Outside this region we have  $D = 0$ . This is true above line 3 because of the formation of a crystal sublattice, and below this line because of the localization of particles in the potential relief of the impurities. The phase diagram found here differs substantially from the high-temperature diagram in Fig. 1.

#### 4. PHASE DIAGRAM FOR $T \neq 0$

Let us examine the changes in the phase diagram with increasing  $T$ , assuming as before that there is no interaction with phonons. In general, the phase diagram is three-dimensional, and we will restrict the discussion to a qualitative look at a few of the most representative cross sections.

Let us consider the case  $y = 0$ . Figure 3 shows the corresponding phase diagram in the  $(x, T)$  plane. In the analysis above it was actually assumed implicitly everywhere that the ratio  $\Delta_0/U_0$  is quite small. When this ratio is nonzero, although small, several different cases are possible, depending primarily on the position of  $x_{cr}$  on the  $x$  axis to the left or right of  $x_c$ . In the latter case, the melting line is as shown by the dashed line in Fig. 3.

In the former case, at  $x < x_{cr}$  (or at  $x < x_c$  in the latter case), the system of particles remains fixed at arbitrary  $T$ . In the interval  $x_{cr} < x < x_c$  the mobility vanishes at all temperatures up to the melting point  $T_m$ , while at  $T > T_m$  the diffusion coefficient is nonzero at all  $T$ .

At  $x > x_c$ , a line (2) appears on the phase diagram which separates the region of self-localization of particles from the region with  $D \neq 0$  (the latter region is the hatched region in Fig. 3). The self-localization depends to a large extent on the random spatial distribution of particles. At  $T \gg U_x$ , a limiting randomization is reached, so that line 2 goes vertically upward with increasing  $T$  as  $x_c - x \rightarrow 0$ . With decreasing  $T$ , in contrast, the degree of randomization decreases, and self-localization sets in at a larger value of  $x$ . With a further decrease in  $T$ , line 2 intersects the melting curve at point  $O$  (or  $O'$ ). To the left of point  $O$  (or  $O'$ ), an extremely nontrivial

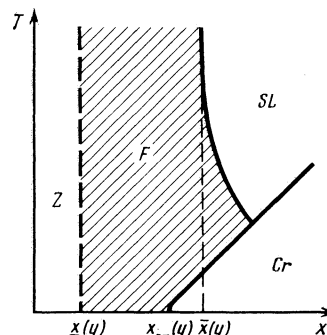


FIG. 4

pattern of phase transitions unfolds with increasing  $T$ . A crystalline phase  $D = 0$  persists up to the melting point; at  $T > T_m$  a liquid phase with  $D \neq 0$  arises, and with a further increase in  $T$  on line 2 this liquid phase transforms into a self-localized phase, again with  $D = 0$ . In the second case, the subsystem of particles remains a liquid with  $D \neq 0$  at  $x_c < x < x'_c$  from  $T = 0$  up to the self-localization line. As a result, localization occurs with increasing temperature in both cases (in the absence of an interaction with phonons). To the right of point  $O$  (or  $O'$ ) the particles are in a self-localized phase as the crystal sublattice melts, so that localization occurs at any  $T$  in this case.

At a fixed value of  $y < y_0$ , the phase diagram in the  $(x, T)$  plane has the same structure as in Fig. 3. Only the reference points change, with  $x_{cr} \rightarrow x_{cr}(y)$  and  $x_c \rightarrow \bar{x}(y)$ . Not until  $y > y_0$  does a fundamental change in structure occur (Fig. 4). In this case, at  $x < \bar{x}(y)$  (Fig. 1), the inelastic interaction between particles is suppressed, and all the one-particle states are localized. We thus find a finite concentration interval  $0 < x < \bar{x}$  (the  $Z$  phase) in which the diffusion coefficient is zero at all  $T$ . With a further increase in  $y$ , the phase diagram remains of the same form as in Fig. 4, but there is a continuous contraction of the liquid region,  $F$ , in which we have  $D \neq 0$ . At  $y > x_c$ , there are no regions with  $D \neq 0$  on the  $(x, T)$  plane.

## 5. CONCLUDING REMARKS

We note first that on these phase diagrams the temperature dependence of the diffusion coefficient in the regions with  $D \neq 0$  may differ greatly, depending on the values of the parameters. The behavior  $D(T)$  can be found in each particular case. At low temperatures, for example, in those parts of region  $F$  in Figs. 3 and 4 which correspond to the localization regime in Fig. 2,  $D$  depends exponentially on the temperature, with an activation energy which varies with  $x$ . Outside the hatched regions, the diffusion coefficient is strictly zero. Only the incorporation of phonons gives rise to a nonzero  $D$ ; at low  $T$  the diffusion coefficient increases with increasing temperature.<sup>2,3</sup>

The  $Z$  phase is of special interest in this connection. In this phase (Figs. 1 and 4) Anderson localization actually persists at a finite density of diffusing particles, at an arbitrary temperature (in the absence of an interaction with phonons). As discussed above, the reasons are the distinctive manner in which inelastic processes are suppressed and the resulting energy diffusion of the particles. In a sense, the problem remains an effectively one-particle problem, and the temperature is responsible only for the distribution of particles among states.

Of particular interest in the diagrams in Figs. 1, 3, and 4 is the self-localized phase  $SL$ . At first glance, this phase is reminiscent of a glass phase, since it is disordered and at the same time has a zero macroscopic diffusion coefficient  $D$ . However, there are some fundamental distinctions between these states. The most important distinction is that the  $SL$  phase is stable, not metastable. Another distinctive feature of this phase is the possible coexistence of static and mobile systems of particles with a macroscopic diffusion coefficient  $D = 0$ . Finally, the short-range order in the  $SL$  phase is

formed in a way completely different from that in a glass.

The entire analysis here has been based on the assumption that the particles interact in accordance with the power law (1), and inequality (2) holds. Narrow bands occur in a natural way in the quantum diffusion of light atomic particles in a crystal. In such cases it is easy to arrange conditions such that  $\Theta_D \gg T \gg \Delta$  (where  $\Theta_D$  is the Debye temperature), so that the effect of the interaction with phonons and thus the phonon-stimulated diffusion are largely suppressed. It was in such a system—in a study of the quantum diffusion of  $\text{He}^3$  atoms in a crystalline  $\text{He}^4$  lattice—that the phenomenon of self-localization was discovered.<sup>4-6</sup> Our analysis has accordingly focused on such systems.

In analyzing the mobility of electrons in crystals in the case of anomalously narrow bands, however, in particular, in the case of a strong polaron effect, we are dealing with a situation in which ratio (2) may actually be small (in this case,  $U_0$  is the Coulomb interaction of the electrons over an interatomic distance). If the screening radius is large in comparison with  $a_0$ , the results given above can also be used to analyze the problem of electron localization. In particular, a self-localization of electrons might be predicted in an ideal crystal with sufficiently narrow bands.

It is easy to see from the phase diagram in Fig. 3 that if the electrons form a Wigner sublattice at a low temperature then the system may be directly in the  $SL$  phase when it melts as  $T$  is raised (line  $ab$ ). This transition will be fundamentally different from an ordinary insulator-metal transition. For example, if the melting point of the sublattice is comparatively low, the conductivity due to the interaction with phonons will increase with increasing  $T$  in the  $SL$  phase, and only after going through a maximum will it begin to decrease with  $T$  (see Refs. 2 and 3, but note that the specific functional dependences on the temperature in those papers have to be changed, since the condition  $\Delta \ll \Theta_D$  does not generally hold).

Interestingly, a similar picture is observed in magnetite, where a well-known electron phase transition occurs at  $T = 110$  K, and extensive experimental data point to a narrow electron band. Mott<sup>10,11</sup> was the first to suggest that the phase which appears upon the melting of the electron sublattice is a "Wigner glass." The ideas in Ref. 2 and in the present paper can be used to formulate an alternative interpretation of this phase.

We note in conclusion that in a magnetic material with a highly anisotropic interaction between spins one should expect the appearance at high temperatures of a phase which is an analog of  $SL$  and  $Z$  phases simultaneously, in which there will be no spin diffusion. This phase arises in cases in which the scatter in the distances between levels for an individual spin exceeds the amplitude for a flip-flop transition by virtue of fluctuations of the self-consistent field [cf. (13)]. An important point is that in this case the spin diffusion is absent not in the limit  $T \rightarrow 0$  but at a high temperature, at which the scatter of levels reaches a certain magnitude.

<sup>1</sup>P. W. Anderson, Phys. Rev. **102**, 1008 (1958).

<sup>2</sup>Yu. Kagan and L. A. Maksimov, Zh. Eksp. Teor. Fiz. **87**, 348 (1984) [Sov. Phys. JETP **60**, 201 (1984)].

- <sup>3</sup>Yu. Kagan and L. A. Maksimov, *Zh. Eksp. Teor. Fiz.* **84**, 792 (1983) [*Sov. Phys. JETP* **57**, 459 (1983)]; *Phys. Lett.* **95A**, 242 (1983).
- <sup>4</sup>V. A. Mikheev, V. A. Maïdanov, and N. P. Mikhin, *Fiz. Nizk. Temp.* **8**, 1000 (1982) [*Sov. J. Low Temp. Phys.* **8**, 505 (1982)].
- <sup>5</sup>V. A. Mikheev, N. P. Mikhin, and V. A. Maïdanov, *Fiz. Nizk. Temp.* **9**, 901 (1983) [*Sov. J. Low Temp. Phys.* **9**, 465 (1983)].
- <sup>6</sup>V. A. Mikheev, V. A. Maïdanov, and N. P. Mikhin, *Solid State Commun.* **48**, 361 (1983).
- <sup>7</sup>B. L. Altshuler, A. G. Aronov, D. E. Khmel'nitskii, and A. I. Larkin, in: *Coherent Effects in Disordered Conductors in Quantum Theory of Solids* (ed. I. M. Lifshits), Mir, Moscow, 1982, p. 70.
- <sup>8</sup>L. Fleishman and P. W. A. Anderson, *Phys. Rev.* **B21**, 2366 (1980).
- <sup>9</sup>B. I. Shklovskii and A. A. Éfros, *Élektronnyye svoïstva legirovannykh poluprovodnikov* (Electronic Properties of Doped Semiconductors), Nauka, Moscow, 1979.
- <sup>10</sup>N. F. Mott, *Festkörperprobleme* **19**, 331 (1979).
- <sup>11</sup>N. F. Mott, *Philos. Mag.* **B42**, 327 (1980).

Translated by Dave Parsons